Elastic cross sections for electron-ketenylidene (C_2O) collisions

M. M. Fujimoto
Departamento de Física, Universidade Federal de Paraná 81531-990, Curitiba, PR, Brazil

M.-T. Lee
Departamento de Química, Universidade Federal de São Carlos 13565-905, São Carlos, SP, Brazil

S. E. Michelin
Departamento de Física, Universidade Federal de Santa Catarina 88040-900, Florianópolis, SC, Brazil
(Received 30 September 2003; revised manuscript received 23 January 2004; published 12 May 2004)

In this work we report on a theoretical study on elastic electron collisions with ketenylidene radicals in the low and intermediate energy range. Calculated differential and momentum transfer cross sections for the $e^- - C_2O$ collision are reported in the (1–500)-eV range. A complex optical potential composed by static, exchange, correlation-polarization plus absorption contributions, derived from a fully molecular wave function, is used to describe the interaction dynamics. The Schwinger variational iterative method combined with the distorted-wave approximation is applied to calculate scattering amplitudes. Comparison made between our calculated cross sections with the theoretical and experimental results for elastic $e^- - N_2O$ collisions has revealed remarkable similarity for incident energies equal to 20 eV and above. Also, two shape resonances located at around 3 eV and 4.5 eV are observed and identified as due to the $^2\Pi$ and the $^4\Pi$ scattering channels, respectively.

DOI: 10.1103/PhysRevA.69.052706 PACS number(s): 34.80.Bm

I. INTRODUCTION

Electron-molecule collisions play an important role in the physical and chemical processes involved in a number of applications, such as lasers [1], gas discharges, plasmas [2], and magneto-hydrodynamic power generation [3]. Interest in electron collisions with highly reactive radicals has also grown recently, in view of their importance in the development of plasma devices as well as in the atmospheric and astrophysical studies. In particular, the ketenylidene (C_2O) radical is an important reaction intermediate in interstellar cloud formation [4–6] and hydrocarbon combustion [7–9]. There is also a growing interest in metal ketenylidene complexes which can facilitate bond formation and cleavage in organometallic chemistry [10–12].

The C_2O radical was identified in a matrix isolation study by Jacox *et al.* [13] using an infrared spectroscopy. In its ground electronic state ($X^3\Sigma^-$), C_2O was suggested to be an asymmetric linear molecule. Devillers and Ramsay [14] obtained the gas phase absorption spectrum of C_2O using flash photolysis. They observed a rotationally resolved spectrum between 500 and 900 nm and assigned it to the $a^3\Pi^- - X^3\Sigma^-$ transition. Spectroscopic constants for both states were also obtained. More recently, Ohshima and Endo [15], using a high resolution microwave spectroscopy, confirmed the structure of the ground state of C_2O.

Because of its application in a number of fields, the knowledge of the electron-C_2O collisional dynamics is certainly of interest. However, there are no such studies, either experimental or theoretical, reported in the literature. Due to its high chemical reactivity, it is very difficult to generate a C_2O radical beam to be interacted with an electron beam, thus experimental studies on electron-C_2O collisions would be a very hard task. In the present work, we report on a theoretical study on elastic electron-C_2O collisions covering a wide incident energy range. More specifically, differential cross sections (DCS's) and momentum transfer cross sections (MTCS's) in the (1–500)-eV energy range are calculated and reported. The present study made use of a complex optical potential to represent the electron-radical interaction, whereas a combination of the Schwinger variational iterative method (SVIM) [16,17] and the distorted-wave approximation (DWA) [18–20] is used to solve the scattering equations. This procedure has already been applied to treat electron scattering by a number of molecules [21–25] and radicals [26–28] and has provided reliable DCS's, integral cross sections (ICS's), and MTCS's over a wide energy range.

The organization of this paper is as follows. In Sec. II we describe briefly the theory used and also some details of the calculation. In Sec. III we present our calculated results.

II. THEORY AND CALCULATION

Details of the SVIM [16,17] and the DWA [18–20] have already been presented previously, and will only be outlined here. Within the fixed-nuclei framework, the electron-molecule scattering dynamics is represented by a complex optical potential,

$$V_{opt}(\vec{r}) = V^{SEP}(\vec{r}) + iV_{ab}(\vec{r}), \tag{1}$$

where the V^{SEP} is the real part of the interaction potential composed by the static (V_{st}), the exchange (V_{ex}) and the correlation-polarization contributions (V_{cp}) whereas V_{ab} is the absorption potential. In our calculation, V_{st} and V_{ex} are derived exactly from a restricted open-shell Hartree-Fock (ROHF) self-consistent-field (SCF) target wave function. A parameter-free model potential introduced by Padial and Norcross [29] is used to account for the correlation-polarization contributions. In this model a short-range corre-

TABLE I. Calculated properties of C_2O.

	Present	Brown *et al.* [35]
Energy (hartree)	−150.512058	−150.510065
r_{CC} (bohr)	2.5908	2.5772
r_{CO} (bohr)	2.1448	2.1205
Dipole moment (D)	1.381	1.380
α_0 (a.u.)	27.3512	
α_2 (a.u.)	13.2130	
IP (eV)	12.0	

lation potential between the scattering and target electrons is defined in an inner interaction region and a long-range polarization potential in an outer region. The first crossing of the correlation and polarization potential curves defines the inner and outer regions. The short-range correlation potential is derived using the target electronic density according to Eq. (9) of Padial and Norcross [29]. In addition, an asymptotic form of the polarization potential is used for the long-range electron-target interactions. Dipole polarizabilities are needed to generate the asymptotic form of V_{cp}. Since there is no experimental and/or theoretical values available in the literature for the C_2O radical, they were calculated in this work at the single- and double-excitation configuration-interaction (CISD) level of approximation. No cutoff or other adjusted parameters are needed in the calculation of V_{cp}.

Although the main features of the absorption effects are known, taking these effects into account in an *ab initio* treatment of electron-molecule scattering is very difficult. For instance, close-coupling calculations would require all discrete and continuum open channels to be included in the open-channel P space, which is computationally unfeasible. In view of the difficulties, the use of the model absorption potential seems to be presently the only practical manner to account for absorption effects into electron-molecule scattering calculations. In this work, a modified version of the quasi-free-scattering model (QFSM), version 3 of Staszewska *et al.* [30], is used to represent the absorption effects. The first version of the QFSM absorption potential derived by Staszewska *et al.* [31] in 1983 is nonempirical, which simulates the effect of all open inelastic channels (excitation and ionization) on the elastic scattering. Its derivation was based on the model originally proposed in nuclear physics by Goldberger [32] and the target was treated as a free-electron gas. Due to the free-electron-gas treatment, it is very difficult to incorporate true target structure and properties into this model. In a subsequent paper [30], the authors proposed two modified semiempirical versions of QFSM in which some target properties, such as the ionization potential and average excitation energy, were incorporated. Despite its semiempirical nature, no adjusted parameters are required in the calculation of the absorption potential. Therefore, it can be used for predictive purposes rather than just for correlation and interpolation of a existing data base. The semiempirical versions of the QFSM absorption potential are given by

$$V_{ab}(\vec{r}) = -\rho(\vec{r})(T_L/2)^{1/2}(8\pi/5k^2k_F^3)H(\alpha+\beta-k_F^2)(A+B+C), \tag{2}$$

where

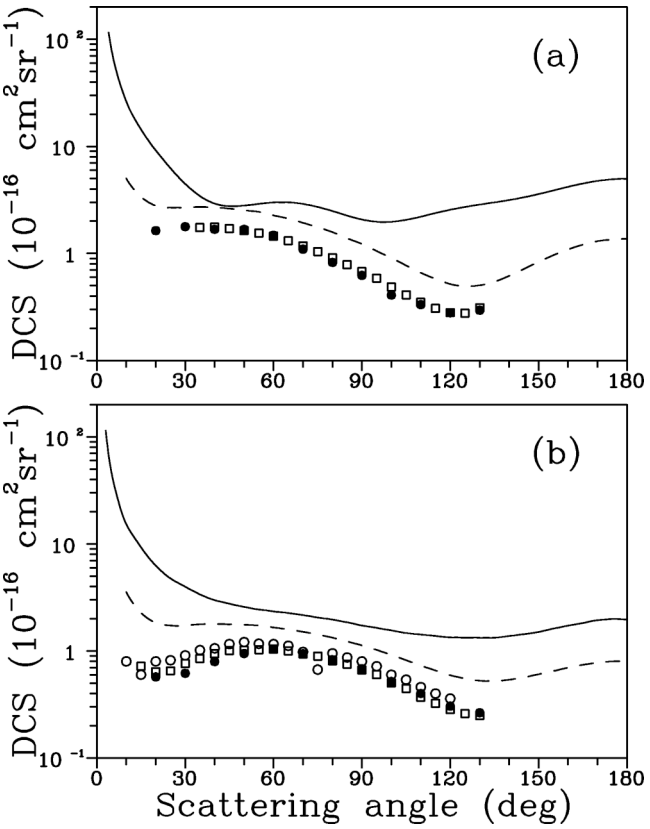

FIG. 1. DCS's for elastic $e^- - C_2O$ scattering at (a) 3 eV and (b) 5 eV. Solid line, present rotationally summed results; dashed line, calculated results for $e^- - N_2O$ scattering [36]. The experimental results for $e^- - N_2O$ scattering are as follows: open squares, Kitajima *et al.* (ANU group) [39]; full circles, Kitajima *et al.* (SU group) [39]; open circles, Johnstone and Newell [38].

$$T_L = k^2 - V^{SEP}, \tag{3}$$

$$A = 5k_F^3/(\alpha - k_F^2), \tag{4}$$

$$B = -k_F^3(5(k^2-\beta)+2k_F^2)/(k^2-\beta)^2, \tag{5}$$

and

$$C = 2H(\alpha+\beta-k^2)\frac{(\alpha+\beta-k^2)^{5/2}}{(k^2-\beta)^2}. \tag{6}$$

In Eqs. (2)–(6), k^2 is the energy (in Rydbergs) of the incident electron, k_F the Fermi momentum, and $\rho(\vec{r})$ the local electronic density of the target. $H(x)$ is a Heaviside function defined by $H(x)=1$ for $x \geqslant 0$ and $H(x)=0$ for $x<0$. According to version 3 of QFSM of Staszewska *et al.* [30],

$$\alpha(\vec{r},E) = k_F^2 + 2(2\,\Delta - I) - V^{SEP} \tag{7}$$

and

$$\beta(\vec{r},E) = k_F^2 + 2(I - \Delta) - V^{SEP}. \tag{8}$$

Here Δ is the average excitation energy and I is the ionization potential. The average excitation energy is a parameter and can be defined [31] as

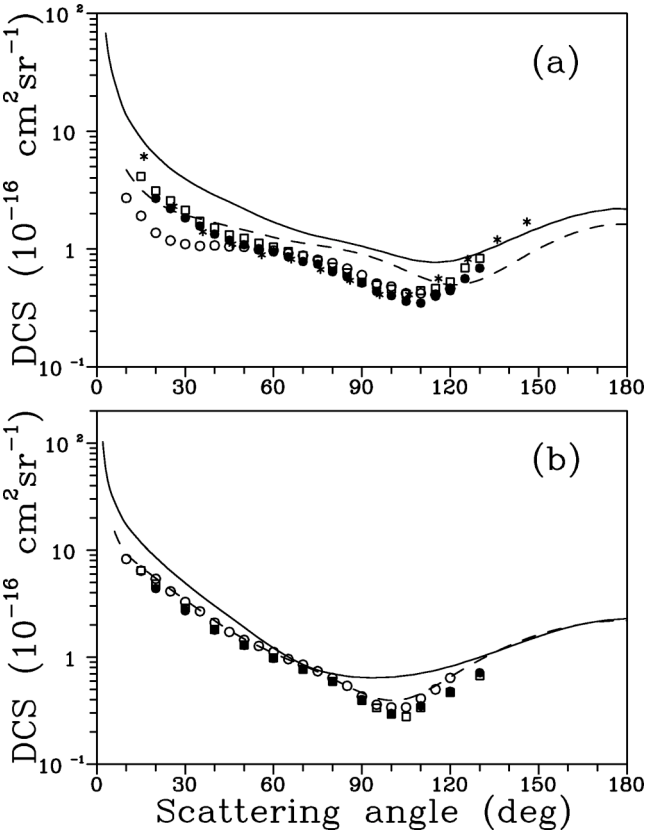

FIG. 2. Same as Fig. 1 except at (a) 10 eV and (b) 15 eV. Stars, experimental data for $e^- - N_2O$ scattering of Marinković *et al.* [37].

$$\Delta = 2\langle \Psi_0 | z^2 | \Psi_0 \rangle / \alpha_0, \tag{9}$$

where Ψ_0 is the ground-state wave function of the target and α_0 the spherical part of the dipole polarizability. In 1991, Jain and Baluja [33] have shown that for a number of molecules, the calculated value of Δ is very close to the ionization potential. Therefore, in the present study, the value of the first ionization potential calculated within a single-excitation CI level of approximation is used as the average excitation energy.

Since C_2O is an open-shell target, the coupling of the incident electron with the two unpaired 2π electrons of the target leads to two spin-specific scattering channels, namely, the doublet ($S=1/2$) and quartet ($S=3/2$) couplings. The main difference between the doublet and quartet scattering channels would reflect on the treatment of the electron-exchange term in the potential operator. On the other hand, contributions such as V_{st}, V_{cp}, and V_{ab} are calculated in the present study using the target electronic density and some molecular properties, such as ionization potential, dipole polarizability, etc. Thus, they are not explicitly dependent on the spin couplings.

Further, the spin-specific Lippmann-Schwinger (LS) equation is solved using the SVIM. In principle, this scattering equation for elastic $e^- - C_2O$ scattering should be solved with the full complex optical potential. Nevertheless, a tremendous computational effort would be required, particularly due to the large number of coupled equations involved,

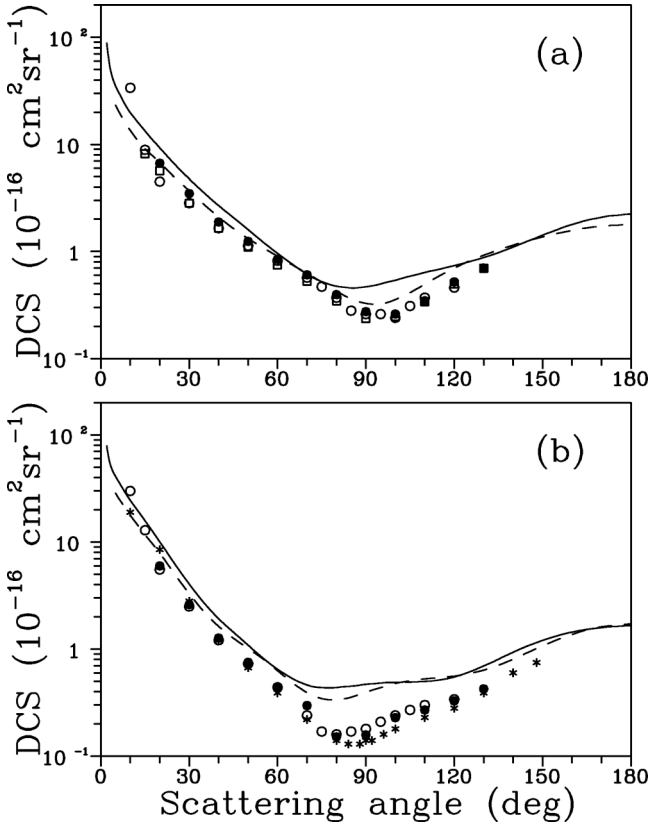

FIG. 3. Same as Fig. 2 except at (a) 20 eV and (b) 30 eV.

which makes such calculations practically prohibitive. On the other hand, our calculation has revealed that the magnitude of the imaginary part (absorption) of the optical potential is considerably smaller than its real counterpart. So, it can be treated as a perturbation. Therefore, in the present study, the LS scattering equations are solved using SVIM considering only the real part of the optical potential. In the SVIM calculations, the continuum wave functions are single-center expanded as

$$\chi_{\vec{k}}^{\pm,S}(\vec{r}) = (2/\pi)^{1/2} \sum_{lm} \frac{(i)^l}{k} \chi_{klm}^{\pm,S}(\vec{r}) Y_{lm}(\hat{k}), \tag{10}$$

where the superscripts (+) and (−) denote the incoming-wave and outgoing-wave boundary conditions, respectively, S is the total spin of the (electron + target) system, and $Y_{lm}(\hat{k})$ are the usual spherical harmonics. The absorption part of the T matrix is calculated via the DWA as

$$T_{abs} = i\langle \chi_f^- | V_{ab} | \chi_i^+ \rangle. \tag{11}$$

In the present work, we have limited the partial-wave expansion of T-matrix elements up to $l_{max}=50$ and $m_{max}=16$. A Born-closure procedure is used to account for the contribution of higher partial-wave dipole components to scattering amplitudes. In order to avoid the divergent behavior of the DCS's in the forward direction, nuclear-rotational dynamics is treated explicitly.

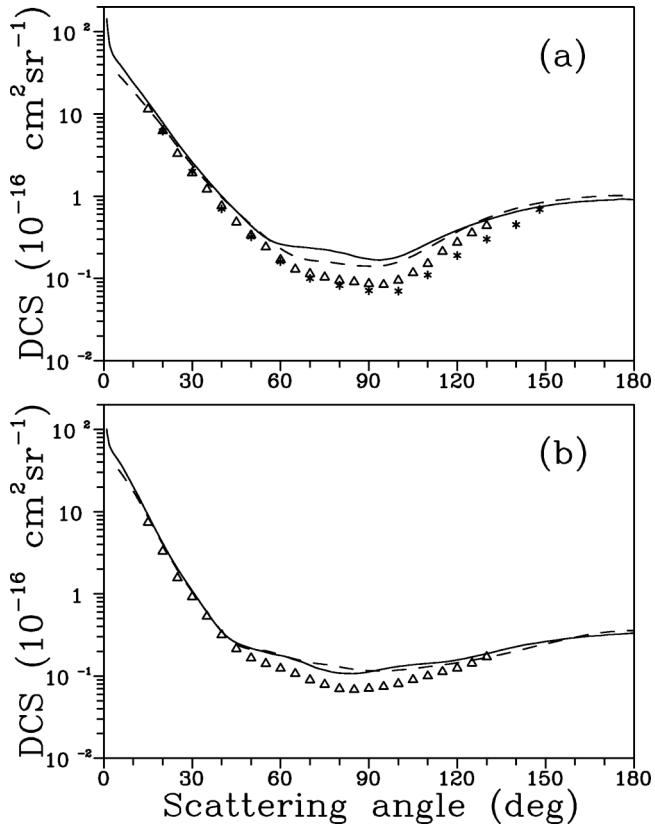

FIG. 4. Same as Fig. 2, except at (a) 50 eV and (b) 100 eV. Open triangles, experimental data for $e^- - N_2O$ scattering of Lee *et al.* [36].

Within the adiabatic-nuclear-rotation (ANR) framework, the spin-specific rotational scattering amplitude is expressed as

$$f^S_{jm_j \leftarrow j_0 m_{j_0}} = \langle jm_j | f^S | j_0 m_{j_0} \rangle, \tag{12}$$

where $|jm_j\rangle$ are the rigid-rotor wave functions and $f^{(S)}$ the spin-specific fixed-nuclear electron scattering amplitude in the laboratory frame (LF). Accordingly, the spin-specific DCS's for the rotational excitation from an initial level j_0 to a final level j is given by

$$\left(\frac{d\sigma}{d\Omega}\right)^S (j \leftarrow j_0) = \frac{k_f}{k_0} \frac{1}{(2j_0+1)} \sum_{m_j m_{j_0}} |f^S_{jm_j \leftarrow j_0 m_{j_0}}|^2, \tag{13}$$

where k_f and k_0 are the final and initial linear momenta of the scattering electron, respectively.

Moreover, the spin-specific rotationally unresolved DCS's for elastic $e^- - C_2O$ scattering are calculated via a summation of rotationally resolved DCS's

$$\left(\frac{d\sigma}{d\Omega}\right)^S = \sum_{j=0} \left(\frac{d\sigma}{d\Omega}\right)^S (j \leftarrow j_0). \tag{14}$$

Finally, the spin-average DCS's for elastic $e^- - C_2O$ scattering is calculated using the statistical weight for doublet (2/6) and quartet (4/6) scattering channels, as

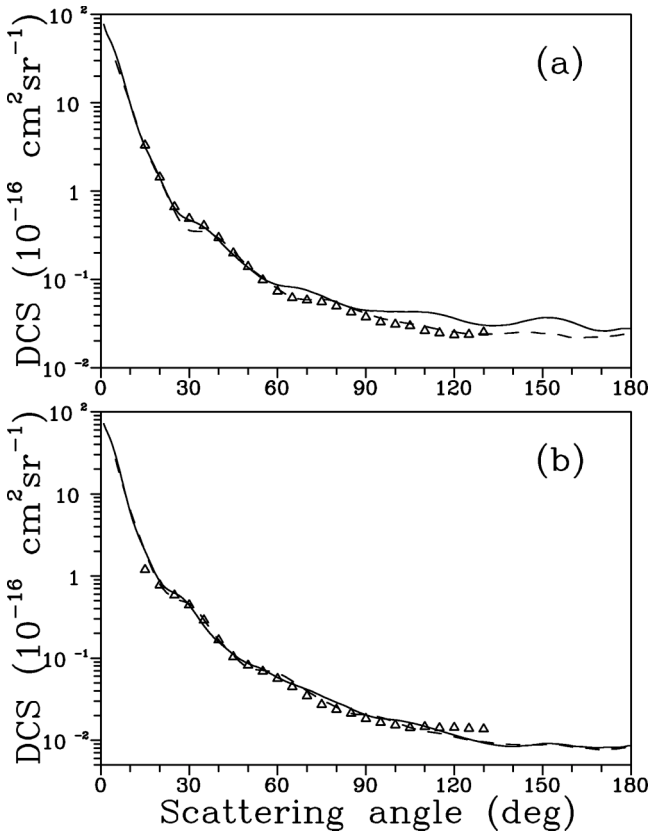

FIG. 5. Same as Fig. 4, except at (a) 300 eV and (b) 500 eV.

$$\left(\frac{d\sigma}{d\Omega}\right) = \frac{1}{6}\left[4\left(\frac{d\sigma}{d\Omega}\right)^{S=3/2} + 2\left(\frac{d\sigma}{d\Omega}\right)^{S=1/2}\right]. \tag{15}$$

In the present study a standard triple-zeta-valence basis set [34], augmented by one $s(\alpha=0.0438)$, one $p(\alpha=0.0438)$, and three $d(\alpha=2.88, 0.72,$ and $0.18)$ uncontracted functions for a carbon atom and one s $(\alpha=0.0845)$, one p $(\alpha=0.0845)$, and three d $(\alpha=5.12, 1.28,$ and $0.32)$ for an oxygen atom, is used for the calculation of the SCF wave function of the target. The results of some calculated properties are summarized in Table I, where the SCF results of Brown *et al.* [35] are also shown for comparison.

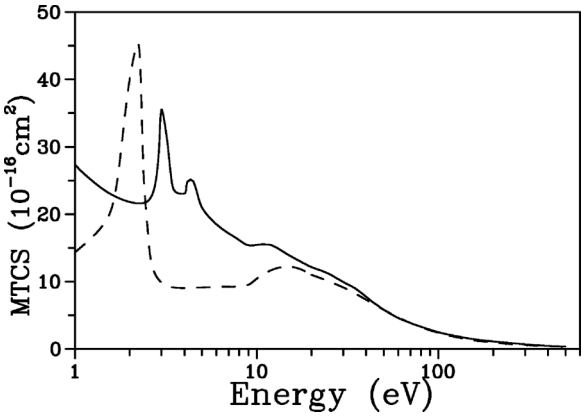

FIG. 6. MTCS's for elastic $e^- - C_2O$ scattering. Solid line, present rotationally summed results; dashed line, calculated results for $e^- - N_2O$ scattering [36].

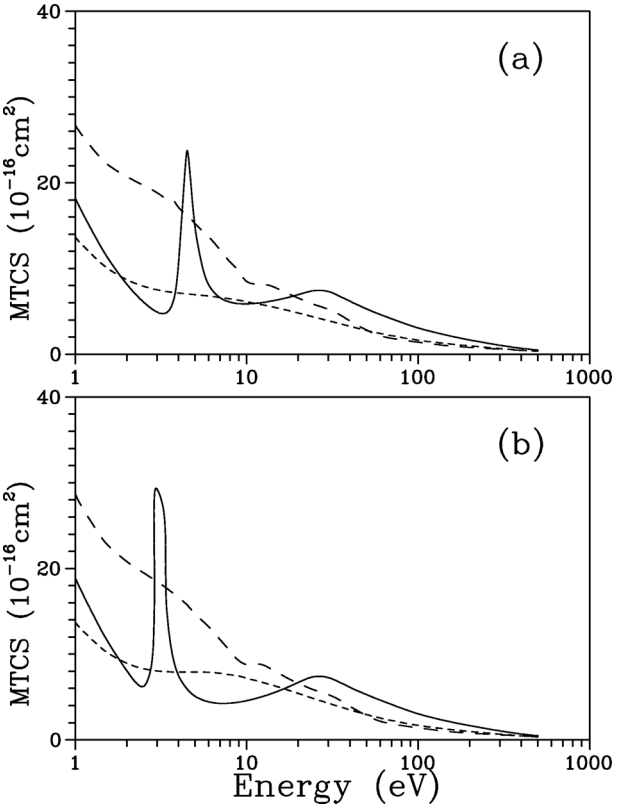

FIG. 7. Partial MTCS's for elastic $e^- - C_2O$ scattering for the (a) dashed line, $^2\Sigma$ scattering channel; solid line, $^2\Pi$ scattering channel; and short-dashed line, $^2\Delta$ scattering channel; (b) dashed line, $^4\Sigma$ scattering channel; solid line, $^4\Pi$ scattering channel; and short-dashed line, $^4\Delta$ scattering channel.

III. RESULTS AND DISCUSSION

In Figs. 1–5 we show our calculated spin-averaged DCS's (rotationally summed) for elastic $e^- - C_2O$ scattering in the (1—500)-eV energy range. Since no experimental or other theoretical results for this target are available in the literature, we use the calculated [36] and measured [36–39] results for elastic $e^- - N_2O$ collisions to compare with our data. This procedure is adopted because N_2O is probably the molecule most similar to C_2O. Thus, we expect that it may provide some insight of the dynamics for the elastic $e^- - C_2O$ collision. At 20 eV and above, the calculated DCS's for electron scattering by C_2O and N_2O are remarkably similar, both qualitatively and quantitatively. This good agreement seems to indicate that the small difference in size (two electrons) between the C_2O and N_2O are not relevant for their interaction with relatively fast electrons. Also, the good agreement between the calculated and experimental DCS's for $e^- - N_2O$ scattering may provide some indications of the reliability of the present study. On the other hand, at lower incident energies the DCS's for $e^- - C_2O$ scattering are considerably larger than those of $e^- - N_2O$ collisions. This is probably due to the fact that the dipole moment of C_2O (1.381 D in the present calculation) is considerably larger than that of N_2O (0.6585 D) [36]. It is well known that the dipole interaction is dominant in electron-molecule scattering at low incident energies.

In view of the possible unreliability of the DCS's near the extremely forward direction due to the use of the ANR approximation, we avoid showing the calculated values of ICS's. On the other hand, the calculation of the MTCS's is less affected and so their reliability is still held. The spin-averaged MTCS's for an elastic $e^- - C_2O$ collision, calculated in the (1—500)-eV range, are shown in Fig. 6. Again, comparison is made with the calculated results for $e^- - N_2O$ scattering [36]. On qualitative aspects, two sharp resonance features located at 3.0 and 4.4 eV, respectively, are clearly seen in the MTCS's for elastic $e^- - C_2O$ collisions. In contrast, only one resonance centered at around 2.0 eV is seen in the MTCS's for $e^- - N_2O$ scattering. In fact, the resonance centered at around 3.0 eV is identified (see Fig. 7) as due to the $^4\Pi$ scattering channel and that located at 4.4 eV is due to the $^2\Pi$ symmetry. The resonance seen in the data for the $e^- - N_2O$ scattering is also due to the $^2\Pi$ symmetry. The shift of about 1.4 eV in the resonance features in C_2O is originated by the different exchange potential operator used in the doublet- and quartet-coupling scattering calculations. It is interesting to note that the effects of this difference only appear significantly near the resonance region. The quantitative comparison between the MTCS's for electron scattering by C_2O and N_2O has revealed very good agreement for incident energies above 20 eV which again confirms the fact that the C_2O radical and N_2O molecules are quite similar for fast electrons. As in DCS's, at lower energies, the MTCS's for $e^- - C_2O$ collision are significantly larger than those of N_2O, except in the resonance region of N_2O.

The appearance of two resonance features in the spin-averaged MTCS's in elastic $e^- - C_2O$ collision, due to the different spin couplings, is indeed very interesting. This fact is also highly relevant because shape resonance constitutes an important mechanism for electron-impact vibrational excitation of molecules. Since different spin couplings can always occur in both natural and artificial environments such as reactive plasmas, where both low-energy electrons and open-shell species are present, they may be important to determine the properties of these environments.

ACKNOWLEDGMENTS

This work was partially supported by the Brazilian agencies FUNPAR, Fundação Araucária, FINEP-PADCT, CNPq, and FAPESP.

[1] S. Trajmar, D. F. Register, and A. Chutjian, Phys. Rep. **97**, 219 (1983).
[2] J. Hahn and C. Junge, Z. Naturforsch. Z. Naturforsch. A **32**, 190 (1977).
[3] W. Wang and N. D. Sze, Nature (London) **286**, 589 (1980).
[4] R. D. Brown, D. M. Craag, P. D. Godfrey, W. M. Irvine, D. McGonagle, and M. Ohishi, Origins Life Evol. Biosphere **21**, 399 (1992).
[5] W. M. Irvine, Adv. Space Res. **15**, 35 (1995).
[6] M. Ohishi, H. Suzuki, S. I. Ishikawa, C. Yamada, H. Kanamori, W. M. Irvine, R. D. Brown, P. D. Godfrey, and N. Kaifu, Astrophys. J. Lett. **380**, L39 (1991).
[7] K. D. Bayes, J. Chem. Phys. **52**, 1093 (1970).
[8] K. H. Becker and K. D. Bayes, J. Chem. Phys. **48**, 653 (1968).
[9] A. Fontijn and S. E. Johnson, J. Chem. Phys. **59**, 6193 (1973).
[10] J. A. Krause-Bauer, J.-H. Chung, E. P. Boyd, J. P. Liu, D. S. Strickland, H.-J. Kneuper, J. R. Shapley, and S. G. Shore, Inorg. Chem. **35**, 1405 (1996).
[11] D. R. Neithamer, R. E. LaPointe, R. A. Wheeler, D. S. Richeson, G. D. Van Duyne, and P. T. Wolczanski, J. Am. Chem. Soc. **111**, 9056 (1989).
[12] D. M. Norton, R. W. Eveland, J. C. Hutchison, C. Stern, and D. F. Shriver, Organometallics **15**, 3916 (1996).
[13] M. E. Jacox, D. E. Milligan, N. G. Moll, and W. E. Thompson, J. Chem. Phys. **43**, 3734 (1965).
[14] M. C. Devillers and D. C. Ramsay, Can. J. Phys. **49**, 2839 (1971).
[15] Y. Ohshima and Y. Endo, J. Chem. Phys. **102**, 1493 (1994).
[16] R. R. Lucchese, G. Raseev, and V. McKoy, Phys. Rev. A **25**, 2572 (1982).
[17] M.-T. Lee, L. M. Brescansin, M. A. P. Lima, L. E. Machado, and E. P. Leal, J. Phys. B **23**, 4331 (1990).
[18] A. W. Fliflet and V. McKoy, Phys. Rev. A **21**, 1863 (1980).
[19] M.-T. Lee and V. McKoy, Phys. Rev. A **28**, 697 (1983).
[20] M.-T. Lee, S. Michelin, L. E. Machado, and L. M. Brescansin, J. Phys. B **26**, L203 (1993).
[21] M.-T. Lee, I. Iga, L. E. Machado, and L. M. Brescansin, Phys. Rev. A **62**, 62710 (2000).
[22] M.-T. Lee and I. Iga, J. Phys. B **32**, 453 (1999).
[23] L. E. Machado, E. M. S. Ribeiro, M.-T. Lee, M. M. Fujimoto, and L. M. Brescansin, Phys. Rev. A **60**, 1199 (1999).
[24] I. Iga, M. G. P. Homem, K. T. Mazon, and M.-T. Lee, J. Phys. B **32**, 4373 (1999).
[25] S. E. Michelin, T. Kroin, I. Iga, M. G. P. Homem, and M.-T. Lee, J. Phys. B **33**, 3293 (2000).
[26] M.-T. Lee, I. Iga, L. M. Brescansin, L. E. Machado, and F. B. C. Machado, Phys. Rev. A **65**, 12720 (2002).
[27] M.-T. Lee, M. F. Lima, A. M. C. Sobrinho, and I. Iga, J. Phys. B **35**, 2437 (2002).
[28] M.-T. Lee, M. F. Lima, A. M. C. Sobrinho, and I. Iga, Phys. Rev. A **66**, 62703 (2002).
[29] N. T. Padial and D. W. Norcross, Phys. Rev. A **29**, 1742 (1984).
[30] G. Staszewska, D. W. Schwenke, and D. G. Truhlar, Phys. Rev. A **29**, 3078 (1984).
[31] G. Staszewska, D. W. Schwenke, D. Thirumalai, and D. G. Trulhar, Phys. Rev. A **28**, 2740 (1983).
[32] M. L. Goldberger, Phys. Rev. **74** 1269 (1948).
[33] A. Jain and K. L. Baluja, Phys. Rev. A **45** 202 (1992).
[34] T. H. Dunning, J. Chem. Phys. **55** 716 (1971).
[35] S. T. Brown, Y. Yamaguchi, and H. F. Schaefer III, J. Phys. Chem. A **104**, 3603 (2000).
[36] M.-T. Lee, I. Iga, M. G. P. Homen, L. E. Machado, and L. M. Brescansin, Phys. Rev. A **65**, 62702 (2002).
[37] B. Marinković, Cz. Szmytkowski, V. Pejčev, D. Filipović, and L. Vušković, J. Phys. B **19**, 2365 (1986).
[38] W. M. Johnstone and W. R. Newell, J. Phys. B **26**, 129 (1993).
[39] M. Kitajima, Y. Sakamoto, R. J. Gulley, M. Hoshino, J. C. Gibson, H. Tanaka, and S. J. Buckman, J. Phys. B **33**, 1687 (2000).